

# Photoinduced switching between charge and orbital ordered insulator and ferromagnetic metal in perovskite manganites

M. Matsubara,<sup>1,\*</sup> Y. Okimoto,<sup>1,†</sup> T. Ogasawara,<sup>1</sup> S. Iwai,<sup>1,‡</sup> Y. Tomioka,<sup>1</sup> H. Okamoto,<sup>1,2</sup> and Y. Tokura<sup>1,3,4</sup>

<sup>1</sup>Correlated Electron Research Center (CERC), National Institute of Advanced Industrial Science and Technology (AIST), Tsukuba 305-8562, Japan

<sup>2</sup>Department of Advanced Materials Science, University of Tokyo, Chiba 277-8561, Japan

<sup>3</sup>Department of Applied Physics, University of Tokyo, Tokyo 113-8656, Japan

<sup>4</sup>Multiferroics Project, ERATO, Japan Science and Technology Corporation, AIST Tsukuba Central 4, Tsukuba 305-8562, Japan

(Received 26 September 2007; revised manuscript received 20 February 2008; published 13 March 2008)

Photoinduced switching in perovskite manganites by irradiation of a femtosecond laser pulse was investigated on  $\text{Pr}_{0.55}(\text{Ca}_{1-y}\text{Sr}_y)_{0.45}\text{MnO}_3$  locating in the critical region between the charge and orbital ordered insulator (CO/OOI) phase and the ferromagnetic metal (FM) phase. For a low excitation density, the charge and orbital order is partially melted and the microscopic quasi-FM domains are generated, which rapidly return to the CO/OOI state. When the excitation density exceeds a threshold, the CO/OOI phase transforms permanently to the FM one. The stabilization of the photoinduced FM state is attributable to the large relaxation of the lattice deformations through the percolation of the microscopic quasi-FM domains.

DOI: 10.1103/PhysRevB.77.094410

PACS number(s): 75.25.+z, 78.20.-e, 75.47.Lx

Ultrafast control of optical, magnetic, and electric properties in solids is an important subject for the developments of future optical-recording or optical-switching devices. Towards this subject, it is necessary to realize the photoinduced change of electron and spin states not through mere sample heating but dominantly through electronic process. A possible way for this is to utilize a photoinduced phase transition (PIPT) in a material showing a bicritical phase competition of an electronic origin.<sup>1</sup> Such a phase competition is prototypically observed in perovskite manganites.<sup>2</sup>

In the perovskite manganites, charge, spin, orbital, and lattice degrees of freedoms are strongly connected to each other, showing various kinds of the electronic phase, such as charge ordered and orbital ordered insulator (CO/OOI), ferromagnetic metal (FM), ferromagnetic insulator, and so on. Recently, the bicritical phase control has been achieved by adjusting the composition very accurately in the manganites such as  $\text{Pr}_{0.55}(\text{Ca}_{1-y}\text{Sr}_y)_{0.45}\text{MnO}_3$  (PCSMO) ( $0 \leq y \leq 1$ ).<sup>3</sup> In PCSMO series, as shown in Fig. 1(a), the end compounds,  $\text{Pr}_{0.55}\text{Ca}_{0.45}\text{MnO}_3$  (PCMO) and  $\text{Pr}_{0.55}\text{Sr}_{0.45}\text{MnO}_3$  (PSMO), are in the CO/OOI phase and FM phase, respectively. This phase change originates from the change in the one-electron bandwidth  $W$  of the  $e_g$  conduction electron; in PCMO with a small  $W$ , the CO/OOI is stabilized by the electron correlation and electron-lattice interactions, while in PSMO with a large  $W$ , the FM is formed by the energy gain through the double-exchange interaction. In PCSMO, a bicritical point between the CO/OOI and the FM phases appears around  $y \sim 0.25$ , as shown in Fig. 1(a).<sup>3</sup> The schematics of the orbital and spin arrangements in the CO/OOI for  $y < 0.25$  (the alternate  $d_{3x^2-r^2}$  and  $d_{3y^2-r^2}$  orbitals and the CE-type antiferromagnetic spins) and in the FM for  $y > 0.25$  are also shown in Fig. 1(a). This material system with the bicritical phase competition is expected to provide a suitable arena to test the ultrafast phase control by photoirradiations. In fact, in the PCSMO thin film, the persistent PIPT from the CO/OOI phase to the FM phase by nanosecond laser excitation has been reported.<sup>4</sup> However, the important information to resolve the mechanism of the

persistent phase transition, such as the dynamical behaviors of the transition and their excitation density dependence, has not yet been clarified.

In this paper, we report on the detailed behaviors of the PIPT induced by the irradiation of a femtosecond laser pulse in single crystals of  $\text{Pr}_{0.55}(\text{Ca}_{1-y}\text{Sr}_y)_{0.45}\text{MnO}_3$  ( $y=0.2-0.24$ ) near the bicritical region between the CO/OOI and the FM phases. The advantage of the study of the bulk single crystal sample is that the solid state properties have been well understood<sup>3</sup> as compared to the film sample, and there is no need of explicit consideration of the substrate effect. We

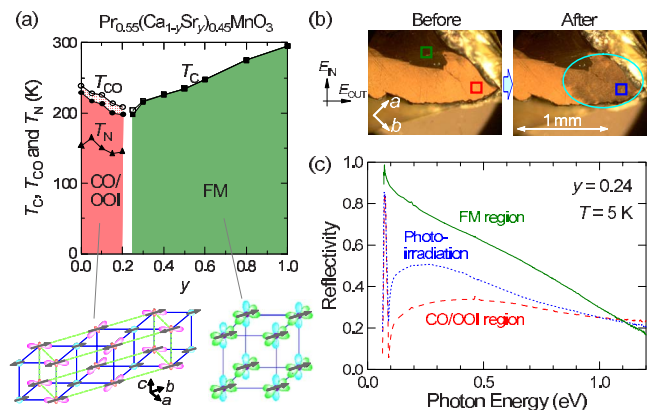


FIG. 1. (Color online) (a) The phase diagram of  $\text{Pr}_{0.55}(\text{Ca}_{1-y}\text{Sr}_y)_{0.45}\text{MnO}_3$  (Ref. 3). The phases of charge and orbital ordered insulator and ferromagnetic metal are denoted as CO/OOI and FM, respectively. Inset: The schematics of the orbital and spin arrangements in the CO/OOI and the FM phases. (b) Polarization microscope images at 30 K for  $y=0.24$  crystal before (the left panel) and after (the right panel) the femtosecond photoexcitation. The dark and the bright regions represent the CO/OOI and the FM states, respectively. The photoirradiated regions are indicated by a circle in the right panel. (c) Reflectivity spectra in the CO/OOI (the broken line), the FM (the solid line), and the photoirradiated (the dotted line) regions at 5 K.

found two characteristic behaviors of the PIPTs depending on the excitation density: the ultrafast photoinduced melting of the CO/OOI state and its recovery and the permanent photoinduced transformation from the CO/OOI state to the FM state. It is pointed out that the lattice relaxations (the release of the deformations) play significant roles in the stabilization of the photoinduced FM phase.

Single crystals of PCSMO were grown by a floating zone method.<sup>3</sup> The specimens were cut from the crystal rod and polished for optical measurements. To remove possible residual strains of the surface due to the polishing procedure, the samples were annealed at 1000 °C in oxygen atmosphere. The reflectivity spectra were measured using a Fourier transform infrared spectrometer equipped with a microscope. For the photoinduced measurements, a Ti:sapphire regenerative amplifier system with the central wavelength of 800 nm (1.55 eV), the pulse width of 100 fs, and the repetition rate of 1 kHz was used as the light source. For the femtosecond pump-probe (PP) spectroscopy, the output of this laser was divided into two beams. One beam (1.55 eV) was used for the pump pulse, and the other for the excitation of an optical parametric amplifier, from which the probe pulses with the range of 0.13–2.0 eV were obtained. Time resolution of the PP system is  $\sim 200$  fs.

Figure 1(b) (the left panel) shows the cross-polarization microscope image of the *ab* plane of a PCSMO ( $y=0.24$ ) single crystal, which is the compound locating on the verge of the boundary between the CO/OOI and the FM phases. The bright and the dark regions represent the CO/OOI and the FM states, respectively. In the region of the CO/OOI state, a bright image is observed through the polarization rotation of the reflection light due to the orbital-ordering-enhanced optical anisotropy in the *ab* plane, while in the region of the FM state, a dark image is obtained because of the nearly isotropic optical response in the *ab* plane.<sup>5</sup> In the  $y=0.24$  crystal, such a macroscopic coexistence of the CO/OOI and the FM phases indicates the nearly degenerate free energy for both states.<sup>6</sup> This bright image was observed to become darker after the irradiation of the Ti:sapphire laser (1.55 eV) with an excitation density of 5 mJ/cm<sup>2</sup>, as indicated by the darkened area surrounded by a circle in Fig. 1(b) (the right panel). This result suggests that in the photoirradiated area, the destruction of the CO/OOI state occurs probably accompanied by the release of the lattice distortions in a macroscopic scale. The photoirradiated area did not return to the initial state even after the temperature was increased up to room temperature. This is in contrast to the photoinduced insulator-metal (IM) transition under electric fields in Pr<sub>0.7</sub>Ca<sub>0.3</sub>MnO<sub>3</sub>, where the metallic region triggered by the pulsed photoexcitation returns to the CO/OOI state upon the removal of the applied voltage.<sup>7,8</sup> It also differs from the photoinduced IM transition in the PCSMO thin film where the metallic state returns to the CO/OOI state through the gentle heating process induced by the irradiation of the cw laser.<sup>4</sup> It should be emphasized that the observed permanent change is not due to the photochemical damage of the sample surface because there are no burnt traces in the microscopic image and the initial bright image due to the CO/OOI state can be completely restored by annealing the sample at 1200 °C.

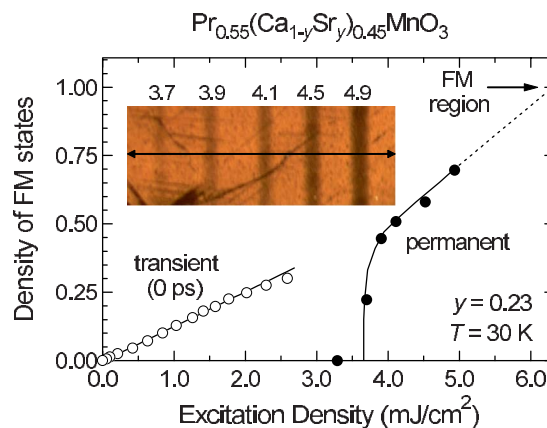


FIG. 2. (Color online) Excitation density dependence of the photoinduced formation of the FM states at 30 K for the  $y=0.23$  crystal (shown by the filled circles). An arrow indicates the intensity of the contrast in the coexistent FM region. The inset shows the polarization microscope image of the photoirradiated bar-shaped area with the different excitation densities. The unit of intensity is mJ/cm<sup>2</sup>. The open circles represent the volume fraction of the photoinduced quasi-FM states immediately after the photoexcitation ( $\sim 0$  ps) estimated from the pump-and-probe measurements for the  $y=0.2$  crystal (see text).

To investigate the variation of the electronic structure by the photoirradiation in more detail, we measured the low-energy reflectivity spectra, which were sensitive to the change of the electronic structure in the course of insulator-metal transition.<sup>9,10</sup> The spectra before and after the photoirradiation are presented in Fig. 1(c). Here, the spectra in the FM, the CO/OOI, and the photoirradiated regions were measured at the positions surrounded by the squares in the left and right panels of Fig. 1(b), respectively. A spiky structure around 0.07 eV is due to an optical phonon mode. After the photoirradiation with 5 mJ/cm<sup>2</sup>, the flat and low reflectivity before the photoirradiation increases, getting closer to the high reflectivity in the FM region. Such a permanent change can be observed only when the excitation density exceeds a threshold value ( $\sim 3.7$  mJ/cm<sup>2</sup>). In the inset of Fig. 2, we show the polarization microscope image around the photoirradiated areas with the excitation densities above the threshold value at 30 K for the  $y=0.23$  crystal. The dark areas that spread out in a longitudinal direction show the photoirradiated regions at different excitation densities. The photoirradiated areas become darker with increasing the excitation density. In Fig. 2, we plotted the intensity of the contrast change with the filled circles as a function of excitation density, which is defined as the decrease of the brightness from the initial anisotropic CO/OOI state. This quantity represents the fraction of the photoinduced FM state, as discussed below. Around the threshold, this quantity reaches about 50%. With the increase of the excitation density above the threshold, the intensity of the contrast change in the photoirradiated area approaches to 1 (the arrow in Fig. 2), i.e., the fully converted FM region. On the other hand, no permanent change was observed below the threshold.

To understand the mechanism of the photoinduced permanent change, it is crucial to investigate its dynamical behav-

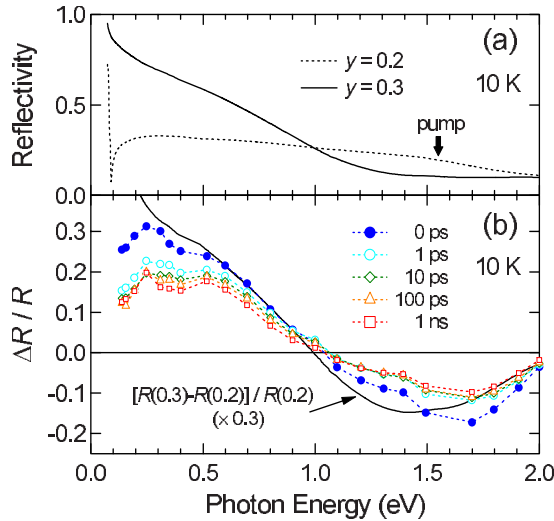


FIG. 3. (Color online) (a) Reflectivity spectra for the  $y=0.2$  (CO/OOI) and the  $y=0.3$  (FM) crystals at 10 K. (b) Reflectivity change  $\Delta R/R$  spectra with  $2.6 \text{ mJ/cm}^2$  for various time delays at 10 K for the  $y=0.2$  crystal. The solid line shows the differential reflectivity spectrum  $\Delta R/R$  between the  $y=0.2$  and the  $y=0.3$  crystals.

ior. Therefore, we performed the femtosecond PP reflection spectroscopy with the excitation densities below the threshold for the  $y=0.2$  crystal.<sup>11</sup> To obtain an overall grasp of the dynamical behavior, first, we show in Fig. 3(b) the spectra of the transient reflectivity change  $\Delta R/R$  at 10 K induced by the photoexcitation ( $2.6 \text{ mJ/cm}^2$ ) for various time delays. The transient reflectivity spectra are similar to the differential reflectivity spectrum [the solid line in Fig. 3(b)] of the  $y=0.2$  (CO/OOI) crystal and the  $y=0.3$  (FM) crystal shown in Fig. 3(a). The  $\Delta R/R$  signal at the delay time  $t_d=0$  ps rapidly decreases in going to  $t_d=1$  ps, while the  $\Delta R/R$  spectra after 1 ps show only a slight difference up to  $t_d=1$  ns.<sup>12</sup> Such a feature can also be clearly seen in the time evolutions of  $\Delta R/R$ . In Fig. 4(a) and its inset,  $\Delta R/R$  at 0.25 eV and 1.5 eV for  $2.6 \text{ mJ/cm}^2$  is presented as a function of  $t_d$ . From these results, we can consider that the time profiles consist of two components, the ultrafast component and the slow component. Taking account of the results of the previous PP measurements on other manganites,<sup>13–20</sup> we assume two exponential decay terms,  $I(t)=I_1e^{-t/\tau_1}+I_2(1-e^{-t/\tau_1})e^{-t/\tau_2}$  (lifetimes  $\tau_1$  and  $\tau_2$ ), for the fast and slow components. The experimental time profiles are well reproduced by this formula, as shown by the solid line in Fig. 4(a). In the fitting procedure, the response function of the measurement system was taken into account. The fast and the slow components are represented by the dotted and broken lines, respectively. The fast component rises instantaneously after the photoexcitation within the time resolution ( $\ll 200$  fs) and decays with the time constant of 0.25 ps. The slow one shows subsequent gradual increase with the relaxation of the first component and then decays slowly. The fast and slow components are ascribed to the melting of CO/OO and its recovery and the heating of the system through the electron-spin-lattice thermalization process, respectively.<sup>13–18</sup> The excitation density

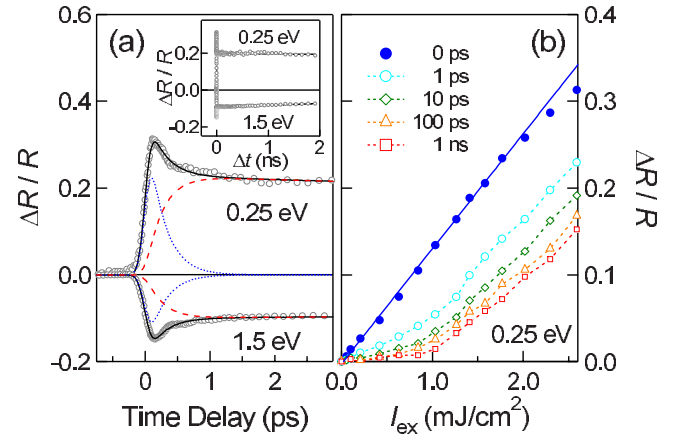


FIG. 4. (Color online) (a) Time evolutions of  $\Delta R/R$  with  $2.6 \text{ mJ/cm}^2$  at 0.25 and 1.5 eV on a fast time scale at 10 K for the  $y=0.2$  crystal. The solid, dotted, and broken lines show the result of fitting (see text). Inset: Time evolutions of  $\Delta R/R$  on a longer time scale. (b) Excitation density dependence of  $\Delta R/R$  at 0.25 eV for various time delays.

dependence of  $\Delta R/R$  at 0.25 eV is shown for various time delays in Fig. 4(b).  $\Delta R/R$  at  $t_d=0$  ps increases linearly with the excitation density, whereas the slower components (1 ps–1 ns) show the nonlinear increase. This result suggests again that the fast and slow components have different origins. Namely, the former corresponds to the formation of the transient microscopic quasi-FM state as described below, while the latter reflects the heating of the system.<sup>17</sup> The relatively large change of the reflectivity by the heating of the system is reasonable, since the CO/OO is sensitive to the temperature and the reflectivity at this probe energy (0.25 eV) considerably increases with the increase of temperature. It has been found that the reflectivity at this probe energy changes nonlinearly against temperature, as described in Ref. 9. This is the reason why the observed reflectivity changes of the slow components show the nonlinear increase against the excitation density or, equivalently, the increase of the temperature of the system. Under the excitation density of  $2.6 \text{ mJ/cm}^2$ , the average number of the absorbed photon is 0.073 per Mn site within the absorption depth of the pump light ( $\sim 65$  nm), which was evaluated by taking account of the reflection loss (20%) and the unit cell volume ( $2.25 \times 10^{-22} \text{ cm}^3$ ). By comparing  $\Delta R/R$  at 0 ps with the differential reflectivity spectrum between  $y=0.2$  and  $y=0.3$ , we can deduce that one excitation photon changes 4–5 Mn sites from the CO/OOI state to the nonordered or quasi-FM state.

On the basis of the results presented above, the ultrafast melting of the CO/OOI state and the permanent transformation to the photoinduced phase can be interpreted as follows. The photoexcitation at 1.55 eV mainly produces a charge transfer excitation from  $\text{Mn}^{3+}$  to  $\text{Mn}^{4+}$ , which should disrupt the CO/OO or, equivalently, the arrangements of the nominally  $\text{Mn}^{3+}$  and  $\text{Mn}^{4+}$  sites and of the staggered  $d_{3x^2-r^2}$  and  $d_{3y^2-r^2}$  orbitals. The resultant delocalization of the  $e_g$  electrons gives rise to the suppression of the electron correlations and electron-lattice interactions responsible for the CO/OO and, instead, may give rise to the competitive FM state in



this bicritical-state manganite. Such an ultrafast formation of a microscopic FM state has been recently demonstrated in the manganite  $\text{Gd}_{0.55}\text{Sr}_{0.45}\text{MnO}_3$  with a short-range CO/OO or, equivalently, a spin glass state.<sup>17,18</sup> However, the local and microscopic FM state can be hardly stabilized. A plausible reason is that the crystal structures, especially the lattice constants, of the FM phase are considerably different from those of the CO/OOI phase; the  $a$  and  $b$  axes in the CO/OOI phase elongate and the  $c$  axis shrinks due to the collective Jahn–Teller distortion arising from the  $e_g$  orbital ordering.<sup>21</sup> Therefore, the large lattice relaxation (the release of the deformation) in the photoirradiated region will be difficult to occur if the excitation density does not reach the threshold. As a result, the microscopic quasi-FM states are transient and rapidly recover to the CO/OO states.

Next, we will discuss in more detail the relation between the transient photoinduced transition and the permanent one. In Fig. 2, we plotted the volume fraction of the transient photoinduced states immediately after the photoexcitation with the open circles, which was estimated by comparing the magnitudes of  $\Delta R/R$  at  $t_d=0$  ps [the filled circles in Fig. 4(b)] with the differential reflectivity spectrum [the solid line in Fig. 3(b)] of the  $y=0.2$  (CO/OOI) crystal and the  $y=0.3$  (FM) crystal. As increasing the excitation density, the fraction of the photoinduced states linearly increases. By assuming that  $\Delta R/R$  at  $t_d=0$  ps increases linearly with the excitation density larger than  $3 \text{ mJ/cm}^2$ , we can deduce that the volume fraction of the transient photoinduced quasi-FM state at the threshold excitation density ( $\sim 3.7 \text{ mJ/cm}^2$ ) is about 50%. Namely, the conversion of the half of the volume fraction would lead to the stabilization of the FM state. The FM domains should be stabilized by connecting with each other. It is, therefore, reasonable to consider that the threshold excitation density corresponds to the percolation threshold of the quasi-FM states. Two-phase coexistence is not discernible in the microscope image of the permanently photoconverted part [see Fig. 1(b)]. This suggests that the characteristic sizes of the FM state and the CO/OOI state is smaller than the wavelength of the visible light. Namely, the continuously connected FM patches with the size of tens or hun-

dreds of nanometers are likely formed in the host of CO/OOI states and cut off the long range CO/OOI state. This is the reason why the reflectivity spectrum of the photoinduced area is not identical with that of the FM one but the intermediate one between the spectra of the two states. Here, it should be noted that the time scales for the transient microscopic melting of the CO/OO states and the permanent transition to the FM states are different from each other. The former is mainly determined by the local dynamics of oxygen ions. Since the period of the stretching mode of the oxygen ions is about 50 fs, the melting of the CO/OO will occur much faster than the time resolution ( $\ll 200$  fs). On the other hand, the lattice relaxation in the permanent transition is associated with the change of the lattice constants on a macroscopic scale. Therefore, it will be rather determined by the sound velocity and take a longer time as compared with the lattice relaxation in the transient microscopic melting. Thus, the percolation of the microscopic FM states and the resultant large lattice relaxation within the FM domains in the host of the CO/OOI states will provide an explanation of the permanent or irreversible PIPT observed in the PCSMO bulk crystal.

In summary, the ultrafast photoinduced melting of the CO/OOI state and the permanent transformation from the CO/OOI to the FM state were observed in the bicritical-state manganites,  $\text{Pr}_{0.55}(\text{Ca}_{1-y}\text{Sr}_y)_{0.45}\text{MnO}_3$  ( $y=0.2-0.24$ ). For a low excitation density, the microscopic melting of the CO/OO or the formation of the quasi-FM domains occurs within the time resolution, but the generated photoinduced phases are unstable and rapidly recover to the CO/OOI state. For the large excitation density above the threshold, on the other hand, the percolative FM patches are permanently formed in the host of CO/OOI states through the release of the lattice distortions. Using the photoinduced transition presented here, it would be possible to pattern nonvolatile FM structures onto the manganites on a wavelength scale of light.

This work was partly supported by a Grant-In-Aid for Scientific Research (Grants Nos. 15104006, 17340104, and 16076205) from the MEXT, Japan.

\*m-matsubara@aist.go.jp

<sup>†</sup>Present address: Department of Materials Science, Tokyo Institute of Technology, Meguro-ku, Tokyo 152-8551, Japan.

<sup>‡</sup>Present address: Department of Physics, Tohoku University, Sendai 980-8578, Japan.

<sup>1</sup>E. Dagotto, *Science* **309**, 257 (2005).

<sup>2</sup>For a recent review, E. Dagotto, *New J. Phys.* **7**, 67 (2005); Y. Tokura, *Rep. Prog. Phys.* **69**, 797 (2006).

<sup>3</sup>Y. Tomioka and Y. Tokura, *Phys. Rev. B* **66**, 104416 (2002).

<sup>4</sup>N. Takubo, Y. Ogimoto, M. Nakamura, H. Tamaru, M. Izumi, and K. Miyano, *Phys. Rev. Lett.* **95**, 017404 (2005); In addition, a persistent photoinduced magnetization has been observed on La or Cr doped  $\text{Pr}_{1-x}\text{Ca}_x\text{MnO}_3$  thin films. See M. Baran, S. L. Gnatchenko, O. Yu. Gorbenko, A. R. Kaul, R. Szymczak, and H. Szymczak, *Phys. Rev. B* **60**, 9244 (1999); Y. Okimoto, Y.

Ogimoto, M. Matsubara, Y. Tomioka, T. Kageyama, T. Hasegawa, H. Koinuma, M. Kawasaki, and Y. Tokura, *Appl. Phys. Lett.* **80**, 1031 (2002).

<sup>5</sup>T. Ishikawa, K. Ookura, and Y. Tokura, *Phys. Rev. B* **59**, 8367 (1999).

<sup>6</sup>It should be noted that the macroscopic phase separation is not basically seen in PCSMO crystals. The coexistence of the CO/OOI state and the FM one observed here is characteristic of the  $y=0.24$  crystal, which locates in the supercritical region between the CO/OOI and the FM phases.

<sup>7</sup>K. Miyano, T. Tanaka, Y. Tomioka, and Y. Tokura, *Phys. Rev. Lett.* **78**, 4257 (1997).

<sup>8</sup>M. Fiebig, K. Miyano, Y. Tomioka, and Y. Tokura, *Science* **280**, 1925 (1998).

<sup>9</sup>Y. Okimoto, Y. Tomioka, Y. Onose, Y. Otsuka, and Y. Tokura,

- Phys. Rev. B **59**, 7401 (1999).
- <sup>10</sup>H. J. Lee, J. H. Jung, K. H. Kim, M. W. Kim, T. W. Noh, Y. Moritomo, Y. J. Wang, and X. Wei, *Physica C* **364-365**, 614 (2001).
- <sup>11</sup>In this  $y=0.2$  crystal, the permanent change was also observed above a threshold just like the aforementioned case of the  $y=0.23$  and  $y=0.24$  crystals.
- <sup>12</sup>Here, 0 ps means the time when  $\Delta R/R$  shows maximum around the time origin, as seen in Fig. 4(a).
- <sup>13</sup>M. Fiebig, K. Miyano, Y. Tomioka, and Y. Tokura, *Appl. Phys. B: Lasers Opt.* **71**, 211 (2000).
- <sup>14</sup>T. Ogasawara, T. Kimura, T. Ishikawa, M. Kuwata-Gonokami, and Y. Tokura, *Phys. Rev. B* **63**, 113105 (2001).
- <sup>15</sup>T. Ogasawara, K. Tobe, T. Kimura, H. Okamoto, and Y. Tokura, *J. Phys. Soc. Jpn.* **71**, 2380 (2002).
- <sup>16</sup>K. Miyasaka, M. Nakamura, Y. Ogimoto, H. Tamaru, and K. Miyano, *Phys. Rev. B* **74**, 012401 (2006).
- <sup>17</sup>Y. Okimoto, H. Matsuzaki, Y. Tomioka, I. Kézsmárki, T. Ogasawara, M. Matsubara, H. Okamoto, and Y. Tokura, *J. Phys. Soc. Jpn.* **76**, 043702 (2007).
- <sup>18</sup>M. Matsubara, Y. Okimoto, T. Ogasawara, Y. Tomioka, H. Okamoto, and Y. Tokura, *Phys. Rev. Lett.* **99**, 207401 (2007).
- <sup>19</sup>R. D. Averitt, A. I. Lobad, C. Kwon, S. A. Trugman, V. K. Thorsmølle, and A. J. Taylor, *Phys. Rev. Lett.* **87**, 017401 (2001).
- <sup>20</sup>S. A. McGill, R. I. Miller, O. N. Torrens, A. Mamchik, I. Wei Chen, and J. M. Kikkawa, *Phys. Rev. Lett.* **93**, 047402 (2004).
- <sup>21</sup>The difference of the lattice constants between  $a$  ( $b$ ) and the  $c/\sqrt{2}$  reaches 2% for the  $y=0.05$  compound (Ref. 3).